NUCLEATION THEORY OF MAGNETIZATION SWITCHING IN NANOSCALE FERROMAGNETS

PER ARNE RIKVOLD[1,2,3], M.A. NOVOTNY[2] AND M. KOLESIK[2]
[1] *Center for Materials Research and Technology,* [2] *Supercomputer Computations Research Institute, and* [3] *Department of Physics*
Florida State University
Tallahassee, FL 32306-3016, USA

AND

HOWARD L. RICHARDS
Max-Planck-Institut für Polymerforschung
D-55128 Mainz, Germany

Abstract. A nucleation picture of magnetization switching in single-domain ferromagnetic nanoparticles with high local anisotropy is discussed. Relevant aspects of nucleation theory are presented, stressing the effects of the particle size on the switching dynamics. The theory is illustrated by Monte Carlo simulations and compared with experiments on single particles.

1. Introduction

The dynamics of magnetization switching in nanometer-sized particles of highly anisotropic ferromagnets is interesting, from both the scientific and technological points of view. The basic scientist sees in such particles a laboratory to study the decay of a metastable phase towards equilibrium, while the technologist sees a promising material for ultrahigh-density magnetic recording media. Although ferromagnetic nanoparticles have been studied experimentally for a long time [1], until recently this was only possible with powders. However, with modern techniques of nanofabrication [2] and ultrahigh-resolution methods to detect the magnetization, such as Magnetic Force Microscopy (MFM) [3] Lorentz microscopy [4] and micro-SQUID devices [5], one can now synthesize and study such particles individually.

The most common description of magnetization switching is a mean-field approach, originally due to Néel [6] and Brown [7]. To avoid an energy barrier due to exchange interactions of strength J, uniform rotation of all the atomic moments in the particle is assumed. The remaining energy barrier, Δ, is caused by magnetic anisotropy, which is a combination of crystal-field and magnetostatic effects. The equilibrium thickness of a wall between oppositely magnetized domains is $\xi \propto \sqrt{J/\Delta}$. For particles smaller than ξ, the uniform-rotation picture is reasonable. If the anisotropy is largely magnetostatic, the resulting demagnetizing field causes particles larger than ξ to form oppositely magnetized domains, and switching is achieved through the field-driven motion of preexisting domain walls. However, if the anisotropy is largely due to the local crystalline environment, there exists a window of particle sizes that are larger than ξ but smaller than the size at which the particle becomes multidomain. [This is for instance often the case in ultrathin films.] Such particles can be modeled as Ising systems with local spin variables, $s_i = \pm 1$. Depending on the degree of anisotropy, these spins can either represent the z component of individual atomic moments, or one can coarse grain the system by rescaling all lengths in terms of ξ, so that the s_i represent block spins. The Ising Hamiltonian is

$$\mathcal{H}_0 = -J \sum_{\langle i,j \rangle} s_i s_j - H \sum_i s_i \ . \tag{1}$$

Here $J > 0$ is the ferromagnetic exchange interaction, H is the applied magnetic field times the local magnetic moment, and the sums $\sum_{\langle i,j \rangle}$ and $\sum_i$ run over all nearest-neighbor pairs and all sites on a suitable lattice, respectively. Here we only report numerical results for two-dimensional square lattices, but our theoretical arguments are valid for general spatial dimension. The order parameter is the dimensionless magnetization,

$$m = N^{-1} \sum_i s_i \ , \tag{2}$$

where N is the total number of Ising spins in the particle.

In the highly anisotropic nanoscale ferromagnets described by Eq. (1) [and modifications discussed below], the state of uniform magnetization opposite to the applied field is properly viewed as a *metastable phase*. This nonequilibrium phase decays by neither uniform rotation nor by the motion of preexisting domain walls, but rather by the thermal nucleation and subsequent growth of *localized droplets*, inside which the magnetization is parallel with the field [8]. This decay mechanism yields results very similar to effects observed in recent experiments on well-characterized single-domain ferromagnets in the nanometer range. In this paper we concentrate on a maximum in the switching field (or coercivity) vs. particle size [3]. Another

quantity which is often measured in experiments, is the probability that the particle has *not* switched within a specified waiting time [4, 5]. Results concerning this quantity can be found in Refs. [8] and [9].

The Ising model does not have an intrinsic dynamic. To simulate the effects of thermal fluctuations we therefore use a local stochastic dynamic which does not conserve the order parameter, such as the ones proposed by Metropolis *et al.* [10] or Glauber [11]. In order to perform simulations on the very long timescales necessary to observe metastable decay, we use a so-called "rejection-free" Monte Carlo (MC) algorithm [12]. The basic time scale of the MC simulation [MC Steps per Spin (MCSS)] is not known from first principles and must be fitted to experiments. It is expected to be on the order of a typical inverse phonon frequency, 10^{-9}–10^{-13} s.

2. Nucleation and Growth

This section is a brief primer on the theory of nucleation and growth as it applies to systems in the dynamic universality class of kinetic Ising models with nonconserved order parameter. For further details, see Refs. [8, 13, 14, 15, 16].

2.1. BACKGROUND

The central problems in nucleation theory are to identify the fluctuations that lead to the decay of the metastable phase and to obtain their free-energy cost, relative to the metastable phase. For Ising-like systems with short-range interactions, these fluctuations are compact droplets of radius R. The magnetization inside the droplet is parallel with the applied field and has a magnitude near the temperature dependent zero-field magnetization, $m_{\rm sp}(T)$, which is nonzero below the critical temperature, T_c. The free energy of the droplet has two competing terms: a positive surface term $\propto R^{d-1}$, and a negative bulk term $\propto |H|R^d$, where d is the spatial dimension. The competition between these terms yields a critical droplet radius,

$$R_c(H,T) = \frac{(d-1)\sigma(T)}{2|H|m_{\rm sp}(T)} \,, \tag{3}$$

where $\sigma(T)$ is the surface tension. Droplets with $R < R_c$ most likely decay, whereas droplets with $R > R_c$ most likely grow further to complete the switching process. The free-energy cost of the critical droplet ($R = R_c$) is

$$\Delta F_{\rm SD}(H,T) = \Omega_d \sigma(T)^d \left(\frac{d-1}{2|H|m_{\rm sp}(T)} \right)^{d-1} , \tag{4}$$

where Ω_d is a weakly T dependent shape factor such that the volume of a droplet of radius R equals $\Omega_d R^d$. The subscript SD stands for Single

Droplet, as explained below. Nucleation is a stochastic process, and the nucleation rate per unit volume is given by a Van't Hoff-Arrhenius relation:

$$I(H,T) \propto |H|^K \exp\left[-\frac{\Delta F_{\rm SD}(H,T)}{k_{\rm B}T}\right] \equiv |H|^K \exp\left[-\frac{\Xi(T)}{k_{\rm B}T|H|^{d-1}}\right] , \quad (5)$$

where $k_{\rm B}$ is Boltzmann's constant, and $\Xi(T)$ is the H-independent part of $\Delta F_{\rm SD}$. The prefactor exponent K equals 3 for the two-dimensional Ising model and $-1/3$ for the three-dimensional Ising model [16, 17, 18].

2.2. EFFECTS OF FINITE PARTICLE SIZE

For particles of finite linear size, L, an important crossover occurs for combinations of H, T, and L, such that $R_c \approx L$. This yields a T and L dependent crossover field called the Thermodynamic Spinodal (ThSp) [15, 16]:

$$H_{\rm ThSp}(T,L) \approx \frac{(d-1)\sigma(T)}{2m_{\rm sp}(T)L} . \quad (6)$$

For $|H| < H_{\rm ThSp}$, R_c would exceed L. This is called the Coexistence (CE) regime because the critical fluctuation in such weak fields resembles two coexisting slabs of opposite magnetization [15, 16]. The average metastable lifetime in the CE regime is approximately

$$\tau_{\rm CE}(H,T,L) \sim \exp\left[\frac{2\sigma(T)L^{d-1} - 2Am_{\rm sp}(T)|H|L^d}{k_{\rm B}T}\right] , \quad (7)$$

where A is a nonuniversal constant. Since $|H| \le H_{\rm ThSp} \sim L^{-1}$, the dominant size dependence is an exponential increase with L^{d-1}. This behavior also holds for more general boundary conditions than the periodic boundary conditions used to obtain Eq. (7) [14].

For $|H| > H_{\rm ThSp}$ (but not too large, as we shall see below), the lifetime is dominated by the inverse of the total nucleation rate,

$$\tau_{\rm SD}(H,T,L) \approx \Big(L^d I(H,T)\Big)^{-1} \propto L^{-d}|H|^K \exp\left[\frac{\Xi(T)}{k_{\rm B}T|H|^{d-1}}\right] . \quad (8)$$

It is inversely proportional to the particle volume, L^d. The subscript SD stands for Single Droplet and indicates that in this regime the switching is completed by the first droplet whose radius exceeds R_c.

A second crossover, called the Dynamic Spinodal (DSp) [15, 16], is predicted when one observes that a supercritical droplet grows at a finite velocity, which for large droplets is proportional to the field: $v \approx \nu|H|$. A reasonable criterion to locate the DSp is that the average time between

nucleation events, $\tau_{\rm SD}$, should equal the time it takes a droplet to grow to a size comparable to L. This leads to the asymptotic relation

$$H_{\rm DSp}(T,L) \sim \frac{(d-1)}{2m_{\rm sp}(T)} \left[\frac{\Omega_d \sigma(T)^d}{(d+1)k_{\rm B}T \ln L} \right]^{\frac{1}{d-1}} . \tag{9}$$

For $|H| > H_{\rm DSp}$, the metastable phase decays through many droplets which nucleate and grow independently in different parts of the system. This is called the Multidroplet (MD) regime [15, 16]. A classical theory of metastable decay in large systems [19, 20, 21] gives the lifetime in this regime,

$$\tau_{\rm MD}(H,T) \approx \left[\frac{I(H,T)\Omega_d (\nu|H|)^d}{(d+1)\ln 2} \right]^{-\frac{1}{d+1}} , \tag{10}$$

which is *independent* of L.

The switching field, $H_{\rm sw}(t_{\rm w},T,L)$, is the field required to observe a specified average lifetime, $t_{\rm w}$. It is found by solving Eqs. (7), (8), and (10) for H with $t_{\rm w}$ for the respective average lifetimes, $\tau_{\rm CE}$, etc. The resulting L dependence of $H_{\rm sw}$ is illustrated by the MC data shown in Fig. 1(a). It consists of a steep increase with L in the CE regime, peaking at the ThSp, followed by a decrease in the SD regime towards a plateau in the MD regime.

3. Numerical Results

In this section we present some representative results of simulations of two-dimensional Ising ferromagnets, which we compare with the theoretical predictions of the previous section and with experiments.

3.1. PURE SYSTEM WITH PERIODIC BOUNDARY CONDITIONS

The simplest model considered is a two-dimensional square-lattice Ising system with periodic boundary conditions. The switching fields for this model at $T = 0.8\,T_c$ are shown in Fig. 1(a) for $t_{\rm w} = 100$ and 1000 MCSS. The L and $t_{\rm w}$ dependencies expected from the results of Sec. 2.2 are clearly seen. We emphasize that the decrease in the SD region is *not* due to an equilibrium domain structure. It is an entropy effect of purely dynamical origin, arising from the volume factor in Eq. (8) [14]. Analogous corrections to nucleation rates in fluids were proposed by Lothe and Pound [22].

For qualitative comparison we show in Fig. 1(b) effective switching fields for nanoscale Ba-ferrite particles, obtained by MFM experiments [3]. We propose that the peak observed in the switching field may be of the same purely dynamical origin as in kinetic Ising models.

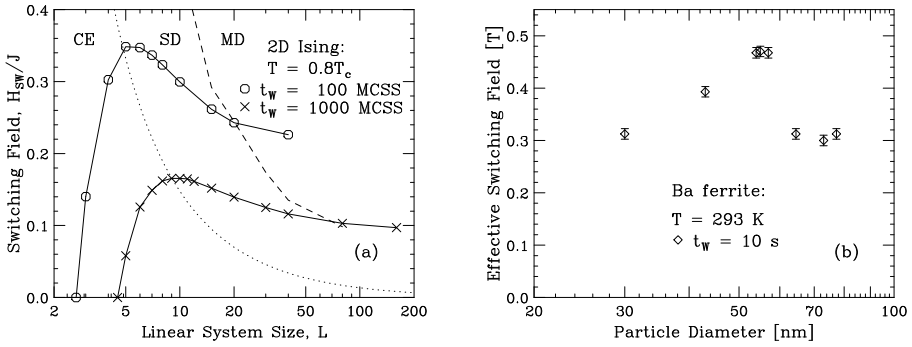

Figure 1. Switching fields vs. particle size. (a): MC simulations for a two-dimensional Ising ferromagnet with periodic boundary conditions. The dotted line is the ThSp, and the dashed line is the DSp. After Ref. [8]. (b): Effective switching fields for nanoscale Ba-ferrite particles. Data digitized from Fig. 5 of Ref. [3].

3.2. EFFECTS OF A DEMAGNETIZING FIELD

A reasonable objection to the model defined by Eq. (1) is the absence of dipolar interactions, which causes it to be single domain for all L. To address this shortcoming without the large computational expense of recalculating dipole sums at every step in the dynamical simulation, a model was introduced in which the demagnetizing field was approximated by adding a weak long-range antiferromagnetic term: $\mathcal{H}_D = \mathcal{H}_0 + DL^d m^2$ [13]. Particles smaller than $L_D \approx 2\sigma(T)/D$ remain single domain [23], but the demagnetizing factor D decreases the free-energy barrier towards nucleation of the equilibrium phase. Addition of the demagnetizing factor was found to reduce the average lifetime by an analytically predictable amount, as shown in Fig. 2. However, no qualitative differences from the behavior described above were observed.

3.3. HETEROGENEOUS NUCLEATION

Next we discuss ways in which the homogeneous nucleation observed in pure systems with periodic boundary conditions is modified by heterogeneous nucleation at the particle surface or at quenched inhomogeneities.

3.3.1. *Modified Boundary Conditions*

The use of periodic boundary conditions allows one to study bulk nucleation without complications due to the particle surface. Since the surface can be modified in various ways by reconstruction, adsorption, oxidation, etc., one cannot in general predict whether it will enhance or inhibit nucleation. However, even addition to the Ising model of a surface field or modified exchange interactions at the surface produces complicated crossovers between

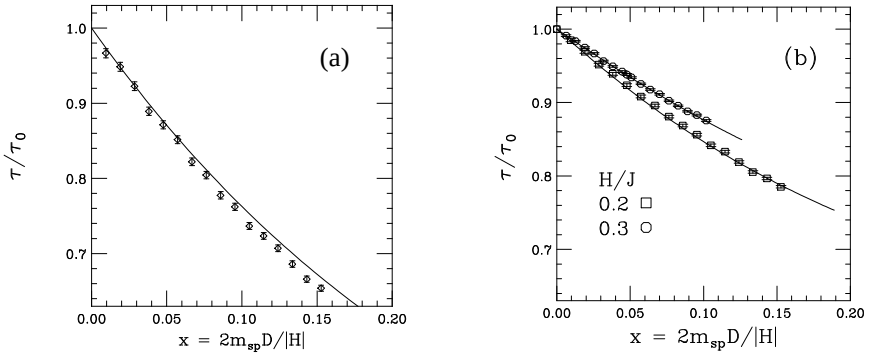

Figure 2. Relative changes in the average metastable lifetime versus the reduced demagnetizing factor, $x = 2Dm_{\rm sp}(T)/|H|$, at $T = 0.8T_c$. The solid curves are analytical results that only require parameters determined for $D = 0$. After Ref. [13]. (a): SD regime, $|H| = 0.2J$, $L = 10$. (b): MD regime, $L = 100$.

surface and bulk nucleation [14]. In general, the changes reduce the height of the peak in $H_{\rm sw}$ vs. L, but for a wide range of modifications it remains clearly discernible. Examples are shown in Fig. 3(a).

3.3.2. *Quenched Randomness*

Another way in which heterogeneous nucleation may dominate, is through quenched impurities. An exploratory study was presented in Ref. [24]. Bond dilution was observed to reduce $H_{\rm sw}$ by a factor approximately independent of L, as shown in Fig. 3(b), while random spin magnitudes led to non-self-averaging behavior and a wide distribution of lifetimes.

3.3.3. *Coercivity of Fe Sesquilayers on W(110)*

Much interest has recently been devoted to ultrathin iron films on W(110) substrates [25, 26, 27, 28, 29]. The so-called sesquilayer systems, which consist of islands of a second monolayer of Fe on top of an almost perfect first monolayer [27], have particularly interesting magnetic properties [28, 29, 30]. Around an Fe coverage of approximately 1.5 monolayers (ML), the coercivity exceeds that of a monolayer or a bilayer by more than an order of magnitude [29].

Magnetization switching in this system is expected to occur through the field-driven motion of preexisting domain walls, which are pinned at the second-layer islands. Based on this picture, the coercivity has been calculated by micromagnetic methods [28, 29]. However, those calculations did not consider thermal effects and were also essentially static.

To account for thermal depinning and the dependence of the coercivity on the frequency of the applied field, a two-layer Ising model has been developed for this system [31]. This is a reasonable approximation since the

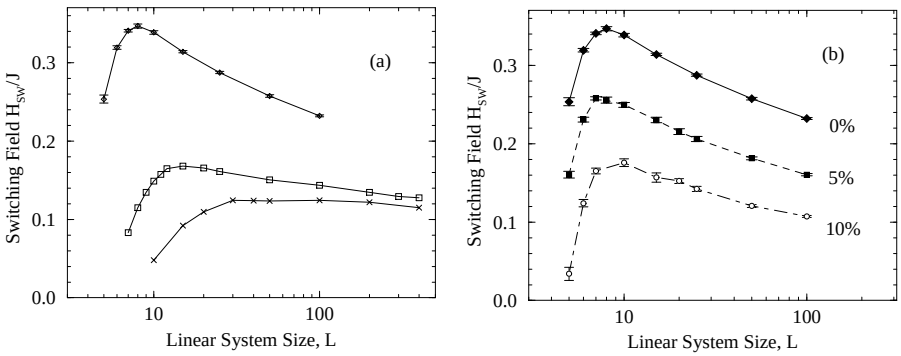

Figure 3. Effects of heterogeneous nucleation on $H_{\rm sw}$ at $T \approx 0.57\,T_c$ with $t_{\rm w} = 30000$ MCSS. For comparison, the top curve in both panels corresponds to homogeneous nucleation in a pure system with periodic boundary conditions. (a): Effects of boundary conditions in a pure system. Middle curve: square system with periodic boundary conditions in one direction and free boundary conditions in the other. Bottom curve: circular system with free boundary conditions. Data from Ref. [14]. (b): Effects of random bond dilution in a system with periodic boundary conditions. After Ref. [24].

crystal-field anisotropy for Fe monolayers on W(110) is almost two orders of magnitude larger than for bulk Fe [25]. Simulations were performed on a computational lattice in which the second-layer island morphology was reproduced using STM images of real systems [27], and the exchange interactions were chosen to reproduce the experimentally observed critical temperature of an Fe monolayer, $T_c = 230$ K [26].

Two simulation snapshots of the magnetic domain wall moving across a sesquilayer are shown in Figs. 4(a) and (b). The wall moves intermittently, spending most of its time pinned against the "windward" side of the islands. Thermally nucleated depinning events are followed by rapid advances to the next metastable position. The coercivity is estimated from the average domain-wall velocity. Estimated coercivities for two different temperatures and driving frequencies are shown vs. the Fe coverage in Fig. 4(c). The experimentally observed nonmonotonic coverage dependence [29] is reproduced, as well as the temperature [28] and frequency [30] dependencies. The model yields an approximately linear dependence of the inverse coercivity on the logarithm of the frequency, shown in Fig. 4(d). Over a few decades of frequency, this is hard to distinguish numerically from a power law [30].

4. Conclusions

We have presented a brief overview of a nucleation theory of magnetization switching in single-domain ferromagnets in the nanometer range. We emphasized the dependence of the switching field or coercivity on the particle size and demonstrated that the model is capable of reproducing the

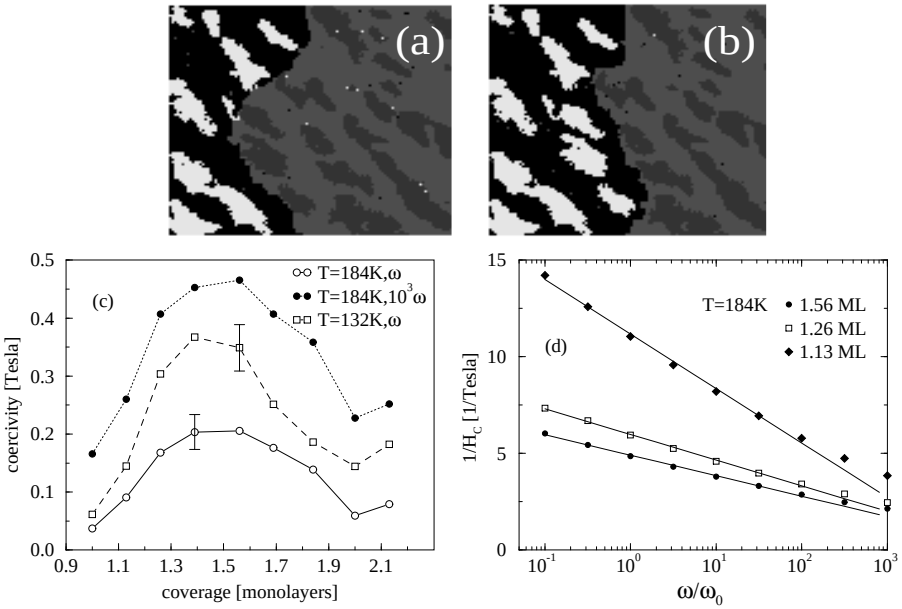

Figure 4. Simulations of magnetization switching in Fe sesquilayers on W(110). After Ref. [31]. (a) and (b): Snapshots of a domain wall propagating across a sesquilayer with coverage 1.26 ML. The high-contrast region represents the growing equilibrium phase. The area shown is 654 Å × 610 Å [109 × 102 computational cells], and the island configuration was digitized from Fig. 1 j) of Ref. [27]. The simulated temperature and field correspond to 132 K and 0.26 T, respectively. The time elapsed between the two snapshots is approximately 1.5×10^6 MCSS, corresponding to 1.5×10^{-6} s. A movie of this simulation is found at `http://www.scri.fsu.edu/~rikvold`. (c): Sesquilayer coercivity vs. Fe coverage, estimated by extrapolation to weak fields. The lower curve should be compared with Fig. 3 of Ref. [29]. (d): The frequency dependence of the estimated coercivity.

experimentally observed maximum in the switching field vs. particle size.

Our discussion places the switching dynamics of nanoscale ferromagnets in the context of metastable decay in finite systems. This interdisciplinary field is experiencing a renaissance due to new methods of nanofabrication and observation of individual systems. In addition to magnets, results have recently been published for systems as different as liquid mixtures [32] and semiconductor nanocrystals [33].

Acknowledgements

Supported in part by Florida State University through the Center for Materials Research and Technology and the Supercomputer Computations Research Institute (Department of Energy Contract DE-FC05-85ER25000), and by National Science Foundation Grants DMR-9520325 and DMR-9315969. Computing resources at the National Energy Research Supercom-

puter Center were provided by the Department of Energy.

References

1. E.F. Kneller and F.E. Luborsky, J. Appl. Phys. **34**, 656 (1963).
2. A.D. Kent, T.M. Shaw, S. von Molnár, and D.D. Awschalom, Science **262**, 1249 (1993).
3. T. Chang, J.-G. Zhu, and J.H. Judy, J. Appl. Phys. **73**, 6716 (1993).
4. C. Salling, S. Schultz, I. McFadyen, and M. Ozaki, IEEE Trans. Magn. **27**, 5184 (1991).
5. W. Wernsdorfer, et al., Phys. Rev. Lett. **78**, 1791 (1997); Phys. Rev. B **55**, 11552 (1997).
6. L. Néel, Ann. Géophys. **5**, 99 (1949).
7. W.F. Brown, J. Appl. Phys. **30**, 130S (1959); Phys. Rev. **130**, 1677 (1963).
8. H.L. Richards, S.W. Sides, M.A. Novotny, and P.A. Rikvold, J. Magn. Magn. Mater. **150**, 37 (1995).
9. M.A. Novotny, M. Kolesik, and P.A. Rikvold, submitted to J. Magn. Magn. Mater.
10. N. Metropolis, A.W. Rosenbluth, M.N. Rosenbluth, A.H. Teller, and E. Teller, J. Chem. Phys. **21**, 1087 (1953).
11. R.J. Glauber, J. Math. Phys. **4**, 294 (1963).
12. M.A. Novotny, Comput. Phys. **9**, 46 (1995); Phys. Rev. Lett. **74**, 1 (1995); erratum **75**, 1424 (1995).
13. H.L. Richards, M.A. Novotny, and P.A. Rikvold, Phys. Rev. B **54**, 4113 (1996).
14. H.L. Richards, M. Kolesik, P.-A. Lindgård, P.A. Rikvold, and M.A. Novotny, Phys. Rev. B **55**, 11521 (1997).
15. H. Tomita and S. Miyashita, Phys. Rev. B **46**, 8886 (1992); P.A. Rikvold, H. Tomita, S. Miyashita, and S.W. Sides, Phys. Rev. E **49**, 5080 (1994).
16. P.A. Rikvold and B.M. Gorman, in *Annual Reviews of Computational Physics I*, edited by D. Stauffer (World Scientific, Singapore, 1994), p. 149.
17. J.S. Langer, Ann. Phys. (N.Y.) **41**, 108 (1967); Ann. Phys. (N.Y.) **54**, 258 (1969).
18. N.J. Günther, D.A. Nicole, and D.J. Wallace, J. Phys. A **13**, 1755 (1980).
19. A.N. Kolmogorov, Bull. Acad. Sci. USSR, Phys. Ser. **1**, 355 (1937).
20. W.A. Johnson and P.A. Mehl, Trans. Am. Inst. Mining and Metallurgical Engineers **135**, 416 (1939).
21. M. Avrami, J. Chem. Phys. **7**, 1103 (1939); **8**, 212 (1940); **9**, 177 (1941).
22. J. Lothe and G.M. Pound, J. Chem. Phys. **36**, 2080 (1962).
23. C. Kittel, Phys. Rev. **70**, 965 (1946).
24. M. Kolesik, H.L. Richards, M.A. Novotny, P.A. Rikvold, and P.-A. Lindgård, J. Appl. Phys. **81**, 5600 (1997).
25. H.J. Elmers and U. Gradmann, Appl. Phys. A **51**, 255 (1990).
26. H.J. Elmers, J. Hauschild, H. Höche, U. Gradmann, H. Bethge, D. Heuer, and U. Köhler, Phys. Rev. Lett. **73**, 898 (1994).
27. H. Bethge, D. Heuer, Ch. Jensen, K. Reshöft, and U. Köhler, Surf. Sci. **331-333**, 878 (1995).
28. D. Sander, R. Skomski, C. Schmidthals, A. Enders, and J. Kirschner, Phys. Rev. Lett. **77**, 2566 (1996).
29. R. Skomski, D. Sander, A. Enders, and J. Kirschner, IEEE Trans. Magn. **32**, 4570 (1996).
30. J.H. Suen and J.L. Erskine, Phys. Rev. Lett. **78**, 3567 (1997).
31. M. Kolesik, M.A. Novotny, and P.A. Rikvold, in preparation.
32. C. Lalaude, J.P. Delville, S. Buil, and A. Ducasse, Phys. Rev. Lett. **78**, 2156 (1997).
33. C.-C. Chen, A.B. Herhold, C.S. Johnson, and A.P. Alivisatos, Science **276**, 398 (1997).